Supporting Information

First-principles study of valley splitting of transition-metal dichalcogenides in MX$_2$/CrI$_3$ (M=W, Mo; X=S, Se, Te) van der Waals heterostructures

Mei Ge,[a] Leiting Chu,[b,c] Fanmin Zeng,[b,c] Zhongyin Cao[b,c*] and Junfeng Zhang [a*]

[a] College of Physics and Electronic Engineering, Hainan Normal University, Haikou 571158, China. E-mail: zhangjf@hainnu.edu.cn (J. Zhang)

[b] Key Laboratory of Spectral Measurement and Analysis of Shanxi Province, Shanxi Normal University, Taiyuan 030031, China.

[c] School of Physics and Information Engineering, Shanxi Normal University, Taiyuan 030031, China. E-mail: caozy@sxnu.edu.cn (Z. Cao)

Considering the mismatch between the different lattice parameters of MX_2 and CrI_3, a twist angle between them is necessary. The red solid line in Fig. S3 indicates the supercell, and $\overset{\shortmid}{a}$ denotes the lattice parameter of the supercell. The lattice vector $\overset{\shortmid}{a}$ may be described in terms of the $\overset{\shortmid}{a} = m\overset{\shortmid}{a}_1 + n\overset{\shortmid}{a}_2$, where $\overset{\shortmid}{a}_1$, $\overset{\shortmid}{a}_2$ are vectors of the unitcell, m, n are chiral index (as shown in Fig. S3). Here, we use θ_{layer} to represent rotated angle between the unitcell vector and supercell vector, which is defined as:

$$\theta_{layer} = arccos\frac{a^2 + (ma_1)^2 - (na_2)^2}{2a(ma_1)}$$

.

The twist angle θ is defined as the difference of the rotated angle for upper and bottom layer. The parameter details corresponding to this work are listed in Table S3 as follows.
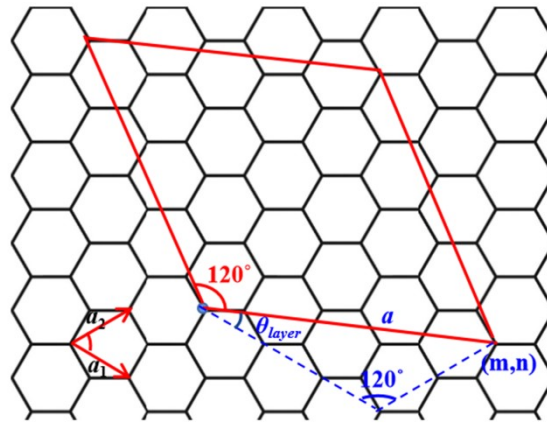

Fig. S1 Schematic diagram of supercell and twist angle.

Table S1 Details of different heterostructures. The $m(n)$, θ_{upper} (θ_{bottom}), θ, δ, l_{upper}, l_{bottom} are chiral indexs, rotated angle for upper (bottom) layer, twist angle of the two layers, lattice mismatch, and lattice of supercell for upper (bottom) layer.

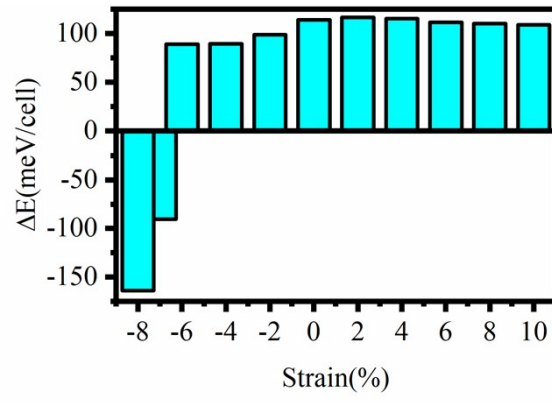|	(m,n) | (m,n)	$\theta_{upper}(°)$ | $\theta_{bottom}(°)$	θ (°)	δ(%)	L_{upper} | l_{bottom}
MoS$_2$/CrI$_3$	(3,2) | (2,0)	23.413 | 0	23.413	1.6	13.774 | 14.004
	(4,0) | (1,1)	0 | 30	30	4.2	12.640 | 12.128
MoSe$_2$/CrI$_3$	(2,0) | (1,0)	0 | 0	0	6	6.58 | 7.002
	(3,1) | (1,1)	13.898 | 30	16.102	2.3	11.851 | 12.128
MoTe$_2$/CrI$_3$	(2,0) | (1,0)	0 | 0	0	0.5	7.04 | 7.002
	(3,1) | (1,1)	13.898 | 30	16.102	4.6	12.692 | 12.128
WS$_2$/CrI$_3$	(4,0) | (1,1)	0 | 30	30	3.9	12.6 | 12.128
WTe$_2$/CrI$_3$	(2,0) | (1,0)	0 | 0	0	1.6	7.12 | 7.002
	(3,1) | (1,1)	13.898 | 30	16.102	5.7	12.825 | 12.128

Fig. S2 Magnetic ground state of monolayer CrI$_3$ under different biaxial strains.

Band properties of two-dimensional (2D) transition-metal dichalcogenides (TMDs) are sensitive to strain. The band structure of free-standing MoS_2 features a direct bandgap. In the MoS2/CrI3 heterostructure with a twist angle of $\theta = 0°$, MoS_2 experiences an 8.4% strain deformation that leads to a direct-to-indirect band transition, as illustrated in Fig. S3(b).
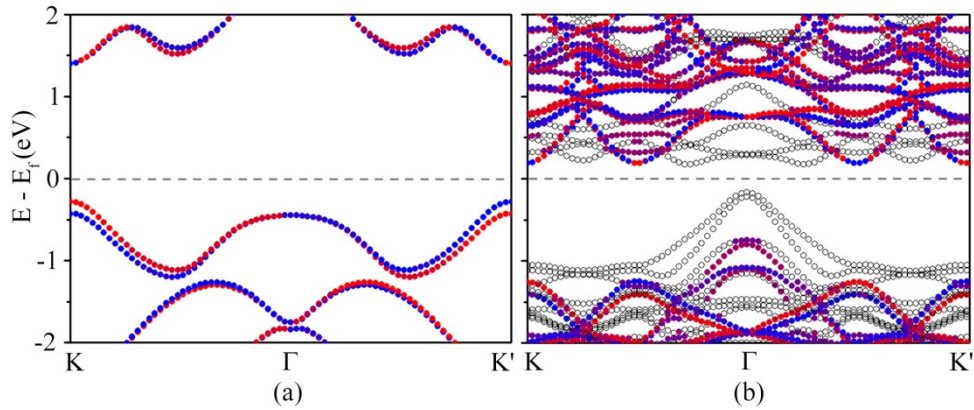

Fig. S3 Electronic structures of monolayer MoS_2 (a) and nontwisted vdW heterostructure MoS_2/CrI_3 (b) with SOC. Red and blue arrows indicate spin-up and spin-down states, respectively. Gray circles are projected bands of CrI_3 layer.

Table S2. Average magnetic moments of Cr ions in 2D vdW heterostructures MX$_2$/CrI$_3$, corresponding to Table 1 in the manuscript.

	a (Å)	θ (°)	Cr_{tot} (μ$_B$)	Cr_s (μ$_B$)	Cr_p (μ$_B$)	Cr_d (μ$_B$)
MoS$_2$/CrI$_3$	13.770	23.413	3.321	0.042	0.048	3.231
	12.570	30	3.302	0.04	0.036	3.225
MoSe$_2$/CrI$_3$	6.660	0	3.29	0.041	0.048	3.20
	11.868	16.102	3.320	0.042	0.048	3.23
MoTe$_2$/CrI$_3$	7.0	0	3.360	0.043	0.048	3.27
	12.527	16.102	3.21	0.037	0.033	3.14
WS$_2$/CrI$_3$	12.556	30	3.395	0.042	0.048	3.30
WTe$_2$/CrI$_3$	7.0	0	3.364	0.043	0.048	3.273

Table S3. Average magnetic moments of Cr ions in 2D vdW heterostructures MX$_2$/CrI$_3$, corresponding to Table 2 in the manuscript.

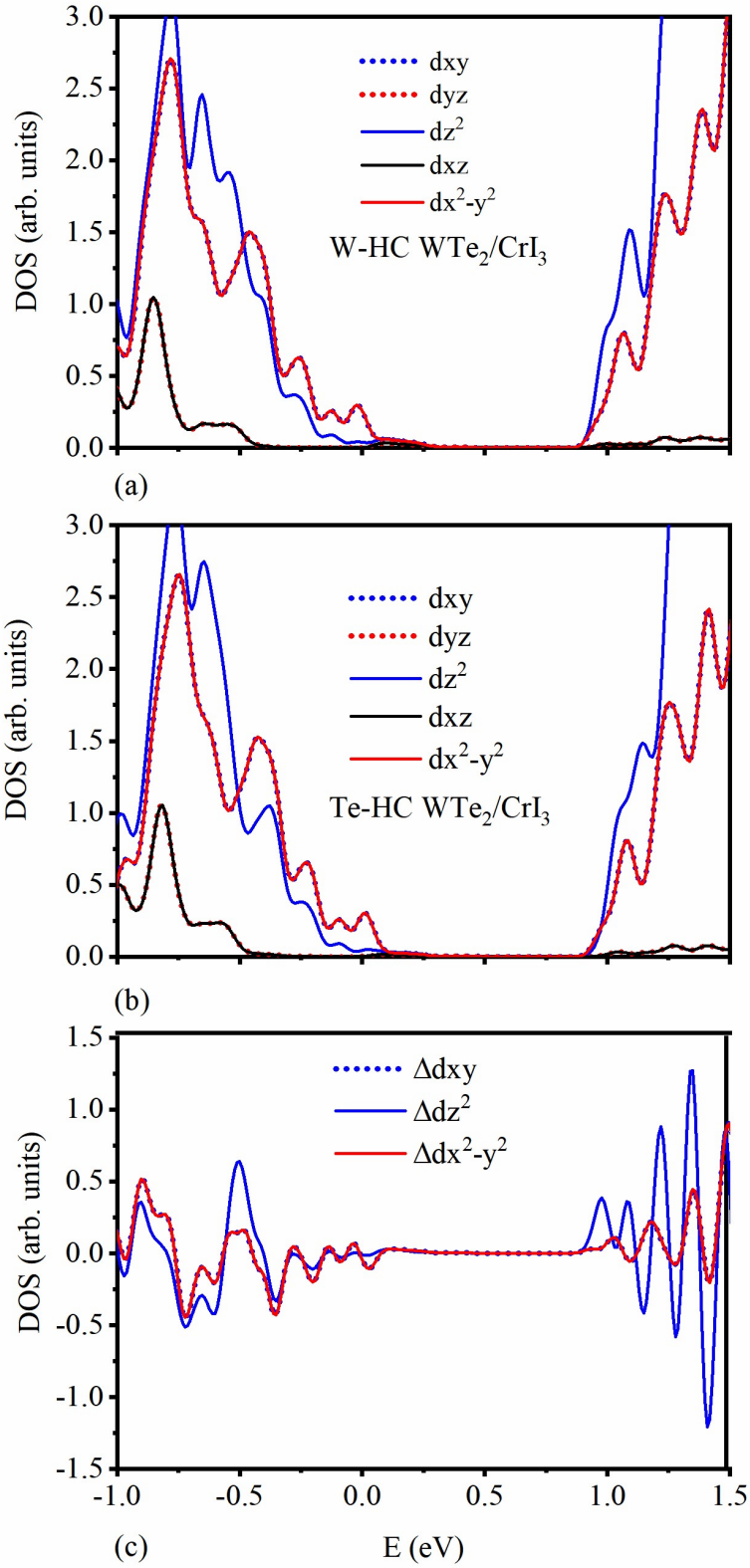|	a (Å)	θ (°)	Cr_{tot} (μ$_B$)	Cr_s (μ$_B$)	Cr_p (μ$_B$)	Cr_d (μ$_B$)
MoS$_2$/CrI$_3$	13.774	23.413	3.322	0.042	0.048	3.232
	12.640	30	3.312	0.04	0.036	3.24
MoSe$_2$/CrI$_3$	6.574	0	3.282	0.041	0.047	3.193
	11.851	16.102	3.316	0.042	0.048	3.226
MoTe$_2$/CrI$_3$	7.004	0	3.175	0.036	0.033	3.105
	12.692	16.102	3.231	0.037	0.033	3.16

Fig. S4 Projected Density-of-States of W atoms in 2D heterostructures (a) W-HC WTe_2/CrI_3, (b) Te-HC WTe_2/CrI_3 and (c) the differences in DOS between (a) and (b) for orbits d_{xy}, d_z^2 and $d_{x^2-y^2}$.